Study of m/n = 1/1 and High-order Harmonic Modes During the Sawtooth Oscillation via 2-D ECEI in a Low β Tokamak Plasma

X.Y. Xu 1), M. Xu 1), J. Wang 1), Y.Z. Wen 1), C.X. Yu 1), B.X. Gao 1), C. Luo 1)
B.N. Wan 2), X. Gao 2)

1) CAS Key Laboratory of Basic Plasma Physics, Department of Modern Physics, University of Science and Technology of China
2) Institute of Plasma Physics, Chinese Academy of Sciences

Email contact of main author: xyxu3@mail.ustc.edu.cn

Abstract The high-order harmonic modes (m,n≥2), along with m = n = 1 mode, in the sawtooth precursor, and the occurrence of the reconnection process during the sawtooth crash have been demonstrated (Plasma Phys. Control. Fusion, **52** (2010) 015008). The harmonics and sawtooth collapse in lower β_p are compared with the theoretical model in further. Assuming constant rotation period on the $q = 1$ radius, circumference images on the $q = 1$ radius are recovered from the rectangular region of ECEI. The rotation period is estimated about T = 240 μs. The time space between the neighboring island is about Δt. The higher-order harmonics can therefore be inferred to be $m = T/\Delta t$ on the $q = 1$ radius. The circumference images show the heat flow collapses through multiple penetration position on the $q = 1$ radius. The wavelet spectrum shows that the frequency of the $m = 1, 2, 3, 4$ is about $f = 4.5, 9, 13.5, 18 kHz$. The high-order harmonic mode is sensitive to the electron density (β_p) and the q profile. It is found that at a fixed q_a value, in the case of low density plasma, the maximum amplitude of the m/n=1/1 mode and the harmonics are about the same; when the density increases above a threshold, the maximum amplitude of the m/n = 1/1 mode significantly increases, while that of the harmonics remains or decreases to a lower level. The threshold $\bar{n}_{e,crit} \propto 1/q_a$ as q_a value increases from $q_a = 2.9$ to $q_a = 4.2$. The dependence of the edge MHD 3/1 mode on the electron density is similar to the 1/1 mode. The 3/1 mode is compared with a stability diagram of the ideal MHD theory. The stability diagram of the ideal MHD mode shows the occurrence of the modes depending on both q_a and q_0 value. The higher q_0 is expected corresponding to higher electron density: $q_0 \propto \bar{n}_e$. Moreover, the density threshold $\bar{n}_{e,crit} \propto 1/q_a$ of the harmonics is reasonable according to the theory. Assuming a monotonically increasing q profile, the stochasticity is predicted to depend on q_0 in some recent investigations (Nucl. Fusion, **47** (2007) 23).

1   Introduction

To understand the mechanism underlying the sawtooth crash, Kadomtsev firstly proposed a 2D full Reconnection model [1]. The model points out the safety factor q is greater than unity inside the q = 1 surface before the sawtooth crash. As the electron temperature increases, once the q_0 on the magnetic axis is lower than 1. The circular hot core will move from the magnetic axis to the q = 1 radius, and reconnection happens there. On the opposite side, a cold crescent island forms simultaneously. As the reconnection processes, the hot core collapses out of the q = 1 radius, accompanying with the crescent island growing, and occupying the region inside the q = 1 radius. And it causes the center q_0 to recover above 1. In large tokamaks, the q_0 not always recover above 1 [2, 3, 4]. And the crash time is much longer than that predicted by the theory.

Along with the contradiction, all kinds of models are proposed. The quasi-interchange model predicts a crescent hot spot and the cooler part of the plasma convects into the core. 3-D
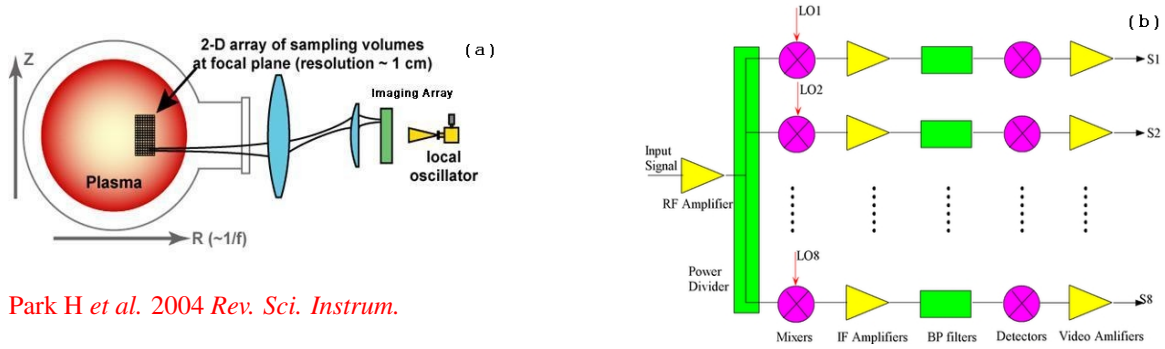
Figure 1: Schematic diagram of the 2-D ECEI optical system and (b) the Intermediate Frequency (IF) System.

reconnection model predicts reconnection occurs at a localized position on the q = 1 radius, the particles and heat collapse out through the reconnection point and therefore it does not change the q profile. [5] Porcelli proposed an incomplete model [6].

High temporal and spatial images of $\Delta T_e/T_e$ during the sawtooth crash are shown using ECEI on TEXTOR. They are compared with the Kadomtsev model and 3-D (ballooning) model. The reconnection indeed occurs. The strong heat flow is observed later than the island establishing. A extremely weak reconnection may occur [7]. The protrusion on the contour line in the image is similar to the pressure finger in the ballooning mode. It excludes the stochastic model, as the flow is highly ordered. The heat flow is also found on the HFS [8], which is not applicable to the character of the ballooning mode. Electron temperature fluctuation of sawtooth crash is investigated by a two dimensional Electron Cyclotron Emission Image technique on the HT-7 tokamak.[9]

High order harmonic modes on q = 1 radius have been observed in low β_p plasmas using different diagnostics in several tokamaks [5, 10, 11, 12, 13]. Using an ECE reconstruction image technique developed on the Tokamak Fusion Test Reactor (TFTR), high-order harmonic modes on q = 1 radius merge into m/n = 1/1 mode before sawtooth crash. A multi-toroidally positioned (MTP) system comprised of three soft x-ray tomography instruments on the WT-3 tokamak reveals the development of the m/n = 2/2 mode and subsequent switch into the m/n = 1/1 mode sawtooth [12, 13]. Utilizing the high-resolution multi-array soft-x-ray emission together with the SVD technique on the HT-7 tokamak, an m/n = 2/2 mode is observed in lower hybrid current drive (LHCD) heating plasmas [14]. Using the technique of ECEI on the HT-7 tokamak, the m/n = 1/1 and its high-order harmonic modes(m/n = 2/2,3/3,...) are observed in sawtooth precursors on the q ~ 1 radius at low density plasma.[9]

2   Setup and Analysis methods

2.1   HT-7 tokamak and ECEI Setup

The experiments are performed in pure ohmic discharges on the HT-7 tokamak, which is a superconducting tokamak with a major radius of 1.22 m, a minor radius 0.27 m, and which employs a circular poloidal limiter. The optical system of the 2-D ECEI (Figure 1) composes of 2 E-plane and 1 H-plane cylindrical lens and 1 spherical substrate lens (3Poloidal mode). An imaging array has 16 receiver/mixers, which is aligned along the vertical (E field) direction. ECE radiation from distinct horizontal plasma chords at about 100GHz focuses onto each element of the imaging array, and then downconverts to achieve IF signal (DC-16GHz)(1st

mixing). The IF signal is then divided into 8 sub-signals and downconverts with 8 distinct LOs. The resultant signal are amplified, bandpass filtered and detected. The resultant effective IF bandwidth (double side band) is 300 MHz. After the 2nd mixing, the ECEI has 8 channels corresponding to 8 narrow discrete band signals from each element of the array.

2.2   ECEI system Characteristic and physics measurements

The 2D ECEI system has high spatial and temporal resolution. As seen in Figure 2, the $1/e^2$ radii of the volumes of the center 13 channels in the vertical (E-plane) direction l_V is 0.9-1.2 cm. The vertical channel spacing d_V is about 1.4 cm, which is for intense focusing with low cross-talk. The spatial resolution is much smaller than the size of modes on the q = 1 radius. In the horizontal direction, the characteristic resolution l_H is about 1 cm, brought by instrument, Doppler shift and relativity radiation broadening. The temporal resolution of the ECEI system is about $4\mu s$, which is abundant for sawtooth crash in about 300 μs. Real time sawtooth oscillation can be studied up to $\sim$ 1% level (the magnitude of the signal noise ratio).

Figure 2: E-pattern resolution of 15 channels (one is dead) corresponding to LO4 in benchmarking.

Generally, using the ECEI system, a 5.6×21 cm (8× 16 channels) image of the electron temperature fluctuation with a temporal resolution of 4 μs in the plasma can be obtained.

ECE radiation is regarded as T_e, as the optic thick is $\tau > 3$ at $n_{e0} = 1.5$ near $r_{q\sim1}$. On the 2D ECEI images, the temperature fluctuation, denoted by $\Delta T_e/\langle T_e \rangle$, is a relative fluctuation on the profile of T_e, represents the heat transfer component on the profile. The bracket $\langle \rangle$ is the time average over many sawtooth oscillations. To observe the reconnection, the ECEI images are selected near the q $\sim$ 1 surface (white arc). It is assumed that the surface with the lowest fluctuation level is the inversion radius, and thus substitutes the q $\sim$ 1 surface.

3   Experimental results

3.1   m/n = 1/1 mode and harmonics during sawtooth oscillation

Using a interpolation method, circumference images of the sawtooth are compared with the 2-D ECEI sequences from [9] in Figure 3. As can be seen, the corresponding rectangular region of the circumference images match the 2-D ECEI sequences very well. The higher harmonics shown in the 2-D ECEI sequences is intuitive in the recovered images. Multiple penetration points exist in the recovered images. The reconnection process during a sawtooth crash is shown. First, a circular hot spot rotates from the bottom to the LFS anticlockwise. Then, at a poloidal location on the isosurface of $\Delta T_e/T_e$, a sharp pressure point is observed near the q $\sim$ 1 radius (-476 μ s), and a finite opening on the contour field line appears (-452 μs). It indicates that, at the poloidal location, there is a local sharp pressure increasing on the magnetic flux, leading the heat to flow out. Multiple openings on q = 1 radius are observed during $-452 \sim -252$ μs. The island establishes completely at 0 μs after the final strong heat flow. The m$\geq$ 4 modes are filtered out a low-pass filter (cutoff frequency 15 kHz) from the images for their
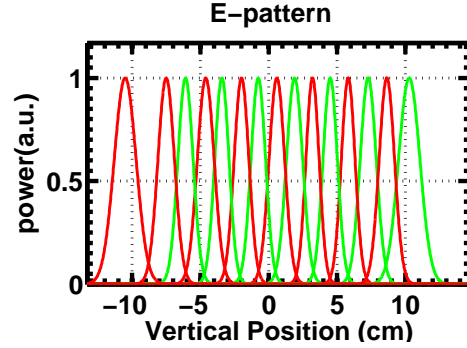
weakness. It is notable that the ECEI circumference images are recovered with the assumptions: the images are on the q = 1 radius, the plasma rotates rigidly and is toroidally symmetry, and the rotation period is assumed constant during the sawtooth oscillation. Generally, from the images, near the location of q = 1, the strong high-order harmonics are observed in the case of low density plasma.
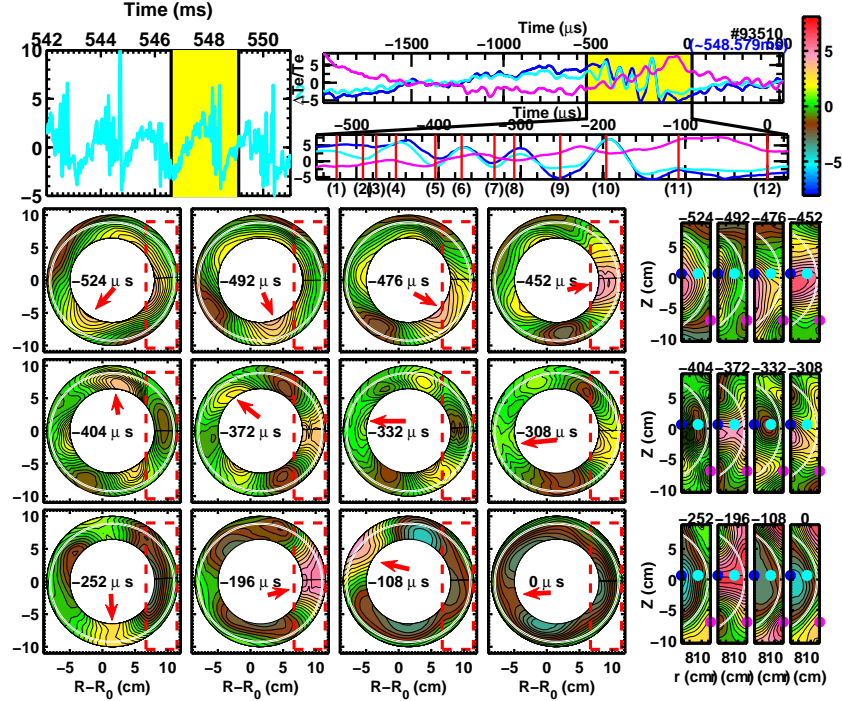

Figure 3: *The recovered circumference images and 2-D ECEI sequence of a typical sawtooth crash with strong m/n = 3/3 mode at about $\bar{n}_{e0} = 1.5 \times 10^{19} m^{-3}$ at $q_a = 3.3$, where the white curves indicate the estimated position of the q ~ 1 surface. Three traces corresponding to the marks on the images below at (r, Z) = (6.7, 0.7), (9.4, 0.7), (11.4, -7) cm , are shown in the top part of the figure.*

The mode number analysis of the harmonics is performed in [9]. Figure 4(a) shows the azimuthal traces of the circumference image. As can be seen, the hot spots propagate $T \sim 220 \mu s$/cycle in the poloidal direction, where T is the rotation period of the plasma. Before the final crash, the harmonics evolve from $m = 3$ to $m \sim 2$ mode at about -300 μs. m = 3 mode is near -400 μs. It corresponds to the strong mode at about 13.5 kHz on the (wavelet) cross-spectrum. During the sawtooth crash phase in Figure 3(a) at about -180 μs, the m = 3 mode evolves to m = 1,2,4 at about 4.5,9,18 kHz.
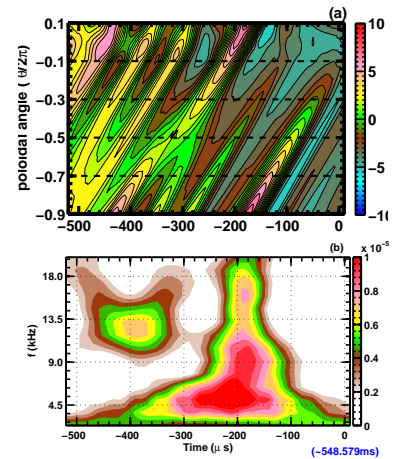

Figure 4: *The contour plot of azimuthal traces. (b)The (wavelet) cross-spectrum of two ECEI signals.*

Based on the fact that the center frequency of the modes is nearly invariant as the density changes, the mode frequency can be expressed as f = 4.5 m kHz, m = 1, 2, 3, 4, ... at $q_a = 3.3$.

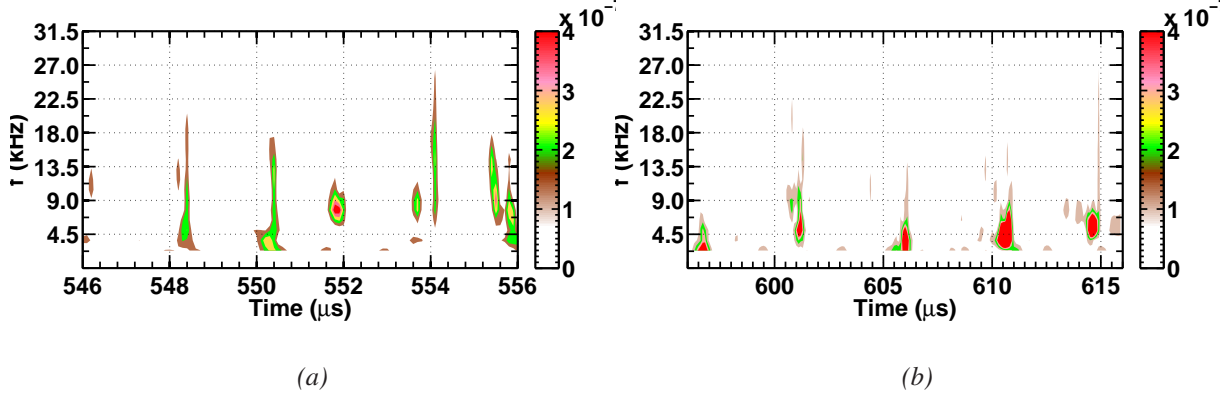*(a)*   *(b)*

Figure 5: The (wavelet) cross-spectrum of two ECEI signals for several sawteeth at (a) low density $\bar{n}_{e0} = 1.5 \times 10^{19} m^{-3}$ and (b) high density $\bar{n}_{e0} = 3.1 \times 10^{19} m^{-3}$.

Figure 5 compares the spectrum at low and high density. As can be seen, at low density, the mode frequency is mainly below 18 kHz. Only a few sawteeth have higher frequency. As a result, using a low-pass filter with a cutoff frequency of 15 kHz is reasonable for 2D images of the sawtooth crash above. While at high density, the frequency is mainly around 4.5 kHz. The harmonics are therefore concluded depending on the electron density. Moreover, the harmonics depend on q_a value, which will be discussed later.

3.2 Parametric study of the amplitude of the modes

As the high-order harmonic mode is sensitive to the electron density (β_p) and the q profile, the amplitude of the 1/1 mode and harmonics are investigated in further in Figure 6 at different density and q_a value. The modes with $m = 1 \sim 4$ are filtered out respectively by a Chebyshev Type II Bandpass Filter with a bandwidth of ± 1 kHz and an attenuation of 20dB outside the band. As can be seen, at $q_a = 3.3$, the 1/1 mode increases dramatically as the density exceeds $\bar{n}_{e0} = 2.5 \times 10^{19} m^{-3}$. The higher harmonics are nearly invariant or decrease a little. It should be a density threshold for the m/n = 1/1 mode and harmonics. The threshold is found to decrease as q_a increases, which we try to understand in the following discussion. In order to understand the harmonics on the $q = 1$ radius, the maximum amplitude of the m/n = 3/1 mode is shown in Figure 6. The 3/1 mode represented in Figure 6 is filtered out using a bandpass filter with a center frequency of 4.5 kHz and bandwidth of $\pm$ 1 kHz using the signal from magnetic probes. As can be seen, the dependence of the edge MHD 3/1 mode on the electron density is similar to the 1/1 mode.

4 Discussion

According to ideal MHD theory, for a circular, large aspect-ratio tokamak with low $\beta (\sim \epsilon^2)$ tokamak ($\beta_p \sim 1$), the complete form of the potential energy of a kink mode perturbation including W_p and W_v in plasma are[15]

$$\delta W = \frac{\pi^2 B_\phi^2}{\mu_0 R} \{ \int_0^a [(r\frac{d\xi}{dr})^2 + (m^2 - 1)\xi^2](\frac{n}{m} - \frac{1}{q})^2 r dr$$
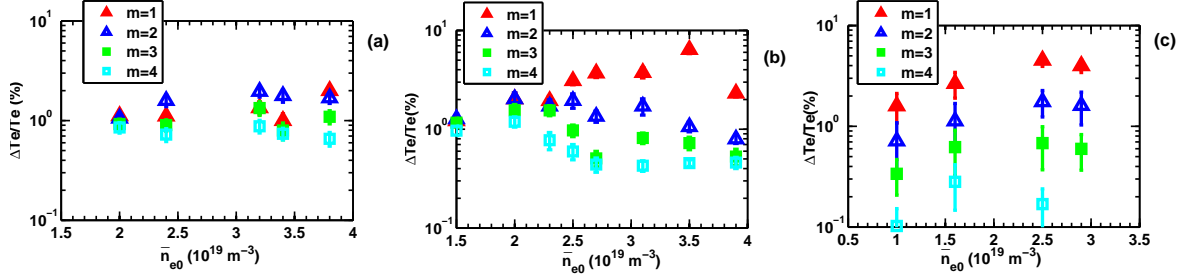$$+ [\frac{2}{q_a}(\frac{n}{m} - \frac{1}{q_a}) + (1 + m\lambda)(\frac{n}{m} - \frac{1}{q_a})^2] a^2 \xi_a^2 \} \qquad (1)$$

Figure 6: *The dependence of the maximum amplitude for the m = 1, 2, 3 and 4 modes ($\Delta T_e/\langle T_e \rangle$) and the m = 3, n = 1 mode (dB_θ/dt) on the electron density at (a) $q_a = 2.9(I_p = 170$ kA, $B_t = 1.665$ T), (b) $q_a = 3.3(I_p = 170$ kA, $B_t = 1.9$ T), and (c) $q_a = 4.2(I_p = 130$ kA, $B_t \sim 1.9$ T). The error bars of $\Delta T_e/\langle T_e \rangle$ represent one fourth of the standard deviation for clear shown ((a) and (b)) and represent the standard deviation ((c)) from dozens of similar sawteeth.*
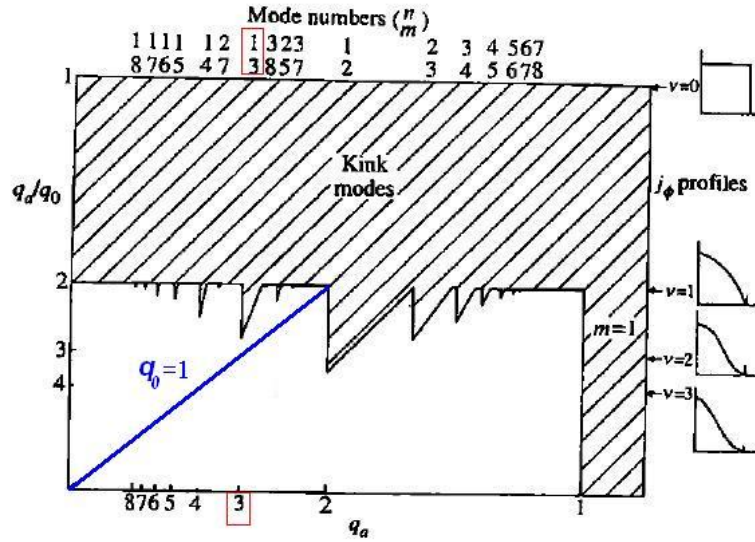

Figure 7: *The stability diagram for kink mode assuming current profile $j = j_0(1 - (r/a)^2)^\nu$. $q_a/q_0 = \nu + 1$*

For $m/n = 3/1$ mode , if $q_a > m/n = 3/1$, $\delta W > 0$, the mode is stable. When $q_a < m/n = 3/1$ slightly, $\delta W < 0$ is possible. Figure 7 shows the stability diagram for Equation (1) with a current distribution $j = j_0(1 - (r/a)^2)^\nu$. The instability at higher q_0 is due to the current profile are steeper near the edge. Several protrusions at the rational surfaces is due to the proximity of the rational surface to plasma from outside.

As seen in Figure 6, for $q_a = 2.9$, as the density increases, the 3/1 mode increases. As seen in Figure 7, for a fixed $q_a = 2.9$ value, the 3/1 mode instability appears at $q_0 > 1$. As q_0 increases, the 3/1 mode increases. It infers $q_0 \propto \bar{n}_e$. Therefore, the lower q_0 value above 1 should cause higher harmonics. However, the reason is still unknown. The protrusion in Figure 7 implies $q_{0,crit} \propto 1/q_a$. It seems consistent with $\bar{n}_{e,crit} \propto 1/q_a$ in Figure 6.

In [16], the q_0 (below 1) dependence of the stochastic is thought important. For conventional tokamak, a monotonically increasing q-profile is assumed. The lower q_0 value causes more low-order rational surfaces and causes more stochastic. On the other hand, in plasmas with ultra flat q profiles, in which $|q(r) - 1| \leq O(\epsilon)$ for $0 \leq r < r_{q=1}$, ideal MHD theory predicts that high harmonics may become unstable if the shear is sufficiently low[17, 18].

5 Summary

2D ECEI on the HT-7 tokamak measures $\Delta T_e / < T_e >$, a relative fluctuation on the profile of T_e, represents the heat transfer component on the profile. It has a high spatial($\sim 1cm <$ island width) and temporal($4\,\mu s \ll t_{crash} \sim 300\,\mu s$) resolution. It provides a partial image on the q = 1 radius with about 1/4 of the poloidal circumference. The m/n = 1/1 mode and high-order(m,n$\geq$2) harmonics in the precursor and the heat flow during the sawtooth crash are investigated deeply. Modes' relationship with the density and q_a are investigated in [9]. A density threshold exists for the modes. At low density, the maximum amplitude of the m/n = 1/1 and harmonics are close. At high density, the m/n = 1/1 mode is prominent. Multiple penetrations at several poloidal position ($\leq$ 3) on the q$\sim$1 radius in the low density plasma are shown, especially evident on the recovered circumference image using an interpolation method. The lower q_0 value above 1 should cause higher harmonics. However, the reason is still unknown. The idea kink mode theory predicts $q_{0,crit} \propto 1/q_a$. It seems consistent with $\bar{n}_{e,crit} \propto 1/q_a$.

6 Acknowledgements

References

[1] Kadomtsev, B.B., Sov. J. Plasma Phys. **1** (1975) 389.

[2] Soltwisch, H., Rev. Sci. Instrum. **59** (1988) 1599.

[3] Levinton, F.M., et al., Phys. Fluids B **5** (1993) 2554.

[4] Yamada, M., et al., Phys. Plasmas **1** (1994) 3269.

[5] Nagayama, Y., Yamada, M., Park, W., Fredrickson, E.D., Janos, A.C., McGuire, K.M., and Taylor, G., Phys. Plasmas **3** (1996) 1647.

[6] Porcelli, F., Plasma Phys. Control. Fusion **38** (1996) 2163.

[7] Park, H.K., Luhmann, N.C., Donné, A.J.H., Classen, I.G.J., Domier, C.W., Mazzucato, E., Munsat, T., van de Pol, M.J., Xia, Z., and TEXTOR team, Phys. Rev. Lett. **96** (2006) 195004.

[8] Park, H.K., Luhmann, N.C., Donné, A.J.H., Classen, I.G.J., Domier C.W., Mazzucato, E., Munsat, T., van de Pol, M.J., Xia, Z., and TEXTOR team, Phys. Rev. Lett. **96** (2006) 195003.

[9] Xu, X.Y., et al., Plasma Phys. Control. Fusion, **52** (2010) 015008.

[10] Sauthoff, N.R., Von Hoeler S. and Stodick W., Nucl. Fusion **18** (1978) 1445.

[11] Nagayama, Y., Taylor G., Yamada M., Fredrickson E.D., Janos A.C., and McGuire K.M., Nucl. Fusion **36** (1996) 521.

[12] Yamaguchi, S., Igami H., Tanaka H. and Maekawa T., Plasma Phys. Control. Fusion **46** (2004) 1163.

[13] Yamaguchi, S., Igami, H., Tanaka, H., and Maekawa, T., Phys. Rev. Lett. **93** (2004) 045005-1.

[14] Sun, Y.W., Wan, B.N., Hu, L.Q., Chen, K.Y., Shen, B. and Mao, J.S., Plasma Phys. Control. Fusion **51** (2009) 065001.

[15] Wesson, J., et al., Tokamaks, Third Edition, Clarendon Press, Oxford (2004), 316-317.

[16] Igochine, V., Dumbrajs, O., Zohm, H., Flaws, A. and the ASDEX Upgrade Team Nucl. Fusion, **47** (2007) 23.

[17] Hastie, R.J. and Hender, T.C., Nucl. Fusion **28** (1988) 585.

[18] Wahlberg, C. and Grave, J., Phys. Plasmas **14** (2007) 110703.